

Supporting Information

Sustaining syngas production at a near-unity H₂/CO ratio in the photo-induced dry reforming of methane independent of the reactant gas composition.

Hiroaki Kaneko,^a Yohei Cho,^a Tomotaka Sugimura,^a Ayako Hashimoto,^b Akira Yamaguchi,^a Masahiro Miyauchi^{*,a}

^a Department of Materials Science and Engineering, School of Materials and Chemical Technology, Tokyo Institute of Technology, 2-12-1 Ookayama, Meguro-ku, Tokyo 152-8552, Japan.

^b National Institute for Materials Science, 1-2-1 Sengen, Tsukuba, Ibaraki 305-0047, Japan.

Contents of Supporting Information

Note 1. Experimental details.

Note 2. Calculation method for thermodynamic equilibrium.

Figure S1. XRD pattern of Rh/STO.

Figure S2. SEM image and its EDS elemental mapping images.

Figure S3. UV-vis DRS of STO and Rh/STO.

Figure S4. Tauc plots of STO and Rh/STO.

Figure S5. Spectrum of a Hg-Xe lamp and that passed through an optical cutoff filter longer than 400 nm

Figure S6. Hydrogen production rates under UV and UV/visible light irradiation.

Figure S7. Temperature dependence on the gas composition under the thermodynamic equilibrium.

Figure S8. The consumption rates of CH₄ and CO₂ and the consumption rates ratio (CH₄ cons./ (CO₂ cons. + CH₄ cons.)) in each reactant gas composition.

Figure S9. Carbon balance before and after the reaction in CH₄/CO₂ = 9.

Figure S10. Raman spectra of the catalysts after being used for 30 min.

Figure S11. TG and DTA results of the catalysts after being used for 30 min in CH₄/CO₂ = 9.

Figure S12. The time-on-stream Q-Mass signals during the reaction in CH₄/CO₂ = 1/9.

Note 1. Experimental details,

Synthesis of Rh/STO

A 200 mg mass of a commercial SrTiO₃ (99 %, Sigma-Aldrich) was introduced into a 20 mL aqueous solution at 80 °C, in which 10.23 mg of RhCl₃·3H₂O (≥ 94 %, Kanto Chemical) was dissolved. This solution was dried to a powder at 70 °C overnight. The powder was treated at 500 °C under a 5 % flow of H₂ in Ar to reduce the Rh species. Subsequently, the powder form of Rh/STO was synthesised. The introduced amount of Rh into the impregnation process was 2.0 wt% versus SrTiO₃.

Characterization of Rh/STO

The amount of Rh loaded on the STO was measured by XRF (Malvern Panalytical Epsilon1). The crystal structure of the catalyst was evaluated using XRD (Rigaku, MiniFlex600-C). The optical absorption properties of the catalysts were recorded using UV-vis DRS (JASCO V-770). The microstructures of the catalysts were observed using TEM (JEOL JEM-ARM200F) and SEM (JEOL JCM-7000). The SEM apparatus was equipped with an energy-dispersive X-ray spectroscopy (EDS) for the elemental analysis.

Evaluation of DRM reactions

Photo-induced and thermal DRM reactions were performed under ambient pressure in a temperature-controlled gas flow chamber with a quartz window (ST Japan Heat Chamber Type-1000). The Rh/STO powder (15 mg) was placed in a porous alumina cup in the reactor chamber, and the inner diameter of the ceramic cup was 5 mm. The catalyst was heated to 150 °C under light irradiation or 800 °C under the dark conditions. The surface temperature of the light-irradiated catalyst was measured by a radiative thermometer (JAPANESE SENSOR, FLHX-TNE0090-0200B003-000) through the quartz window of the chamber. The composition of the input gas mixture varied between CH₄/CO₂ values of 1/9, 1/4, 1/2, 1, 2, 4, 9, where the total volume of CH₄ and CO₂ was 1 % in Ar. The flow rate of the introduced DRM gas was 15 mL min⁻¹. The concentration of the outlet gas was evaluated using gas chromatography with a thermal conductivity detector (GC-TCD, Agilent 490 Micro GC). The light source was a 150 W Hg–Xe lamp (Hayashi-Repic LA-410UV-5). Light irradiance (2.4 W cm⁻²) was measured using a spectral radiometer (USHIO USR-45).

Raman spectroscopy (JASCO PR-1w) and thermogravimetry-differential thermal analysis (TG-DTA, NETZSCH STA 2500 Reguls) were performed to analyse the carbon depositions after

photo-induced and thermal reactions under a reactant gas composition of $\text{CH}_4/\text{CO}_2 = 9$ for 30 min. For Raman spectroscopy, a 785 nm, 5 mW laser was used for excitation. The wavenumber resolution was $3 \text{ cm}^{-1}/\text{pixel}$ and the scanning range was $2500\text{--}500 \text{ cm}^{-1}$ with an average of 100 scans. The measured spectra were baseline-corrected. For TG-DTA, the sample was heated at a rate of 20 K min^{-1} from $25 \text{ }^\circ\text{C}$ to $700 \text{ }^\circ\text{C}$ under a flowing gas mixture of $\text{O}_2 + \text{N}_2$ (22 %, 78 %) at 90 mL min^{-1} .

An online Q-Mass spectrometer (Q-Mass, ULVAC Qulee BGM-102) was used to analyse the water production during the photo-induced and thermal reactions under the reactant gas composition of $\text{CH}_4/\text{CO}_2 = 1/9$. The flow rate was consistent with the catalytic tests.

Note 2. Calculation method for thermodynamic equilibrium

Thermodynamic equilibrium was calculated using the Chemical Equilibrium with Applications program (CEA), developed by the Glenn Research Center of NASA. For the calculation, the temperature was set at $800 \text{ }^\circ\text{C}$, and the pressure was 1 atm under the various DRM gas compositions similar to the catalyst test ($\text{CH}_4/\text{CO}_2 = 1/9, 1/4, 1/2, 1, 2, 4, 9$).

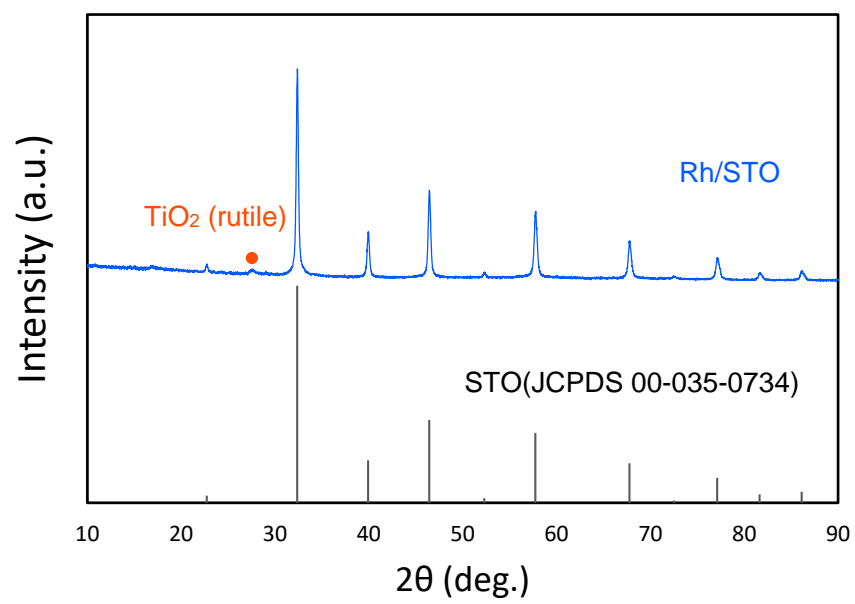


Figure S1. XRD pattern of Rh/STO.

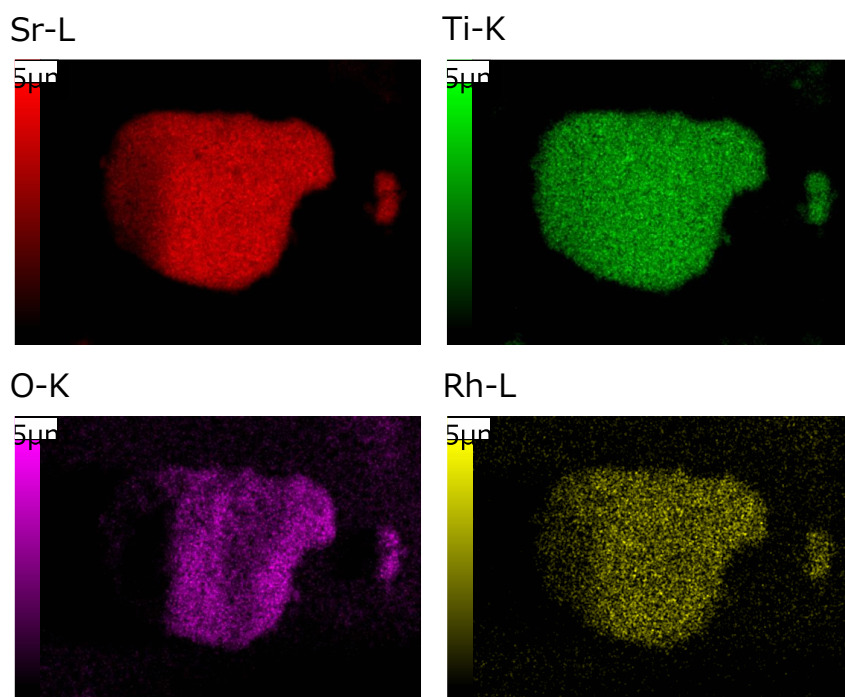
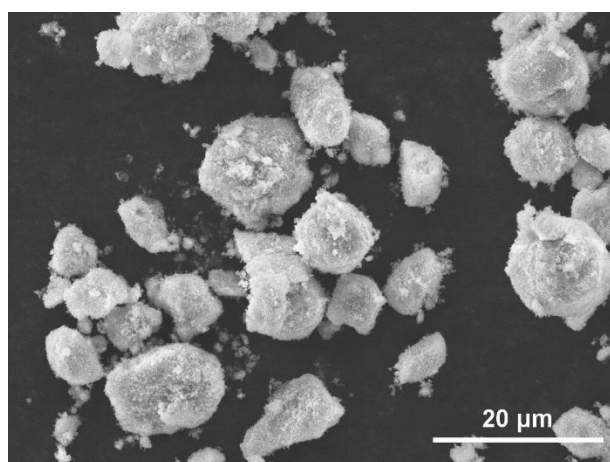


Figure S2. SEM image and its EDS elemental mapping images for strontium (Sr), titanium (Ti), oxygen (O), and rhodium (Rh), respectively.

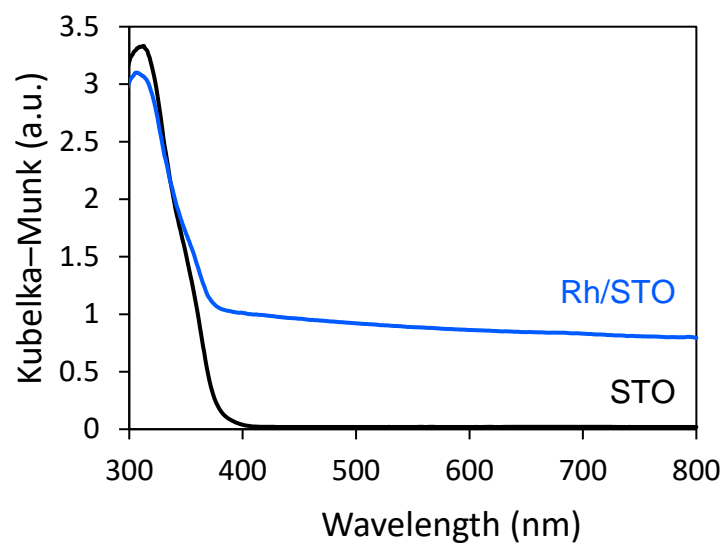


Figure S3. UV-vis DRS of STO and Rh/STO.

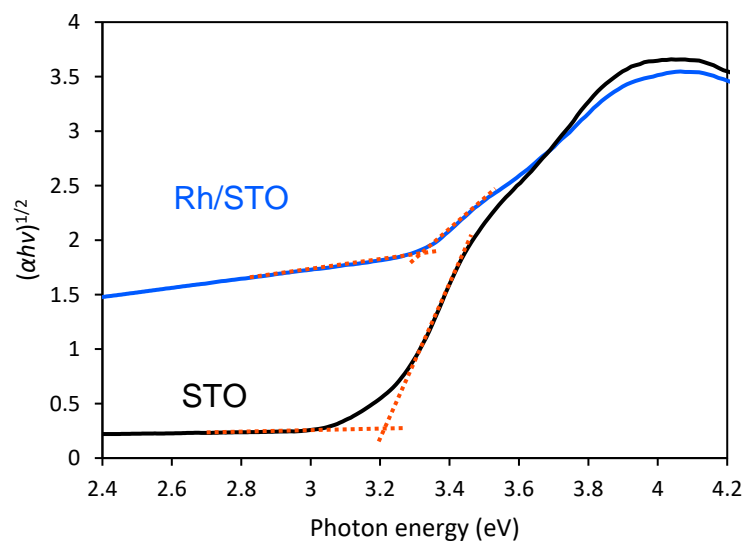


Figure S4. Tauc plots of STO and Rh/STO.

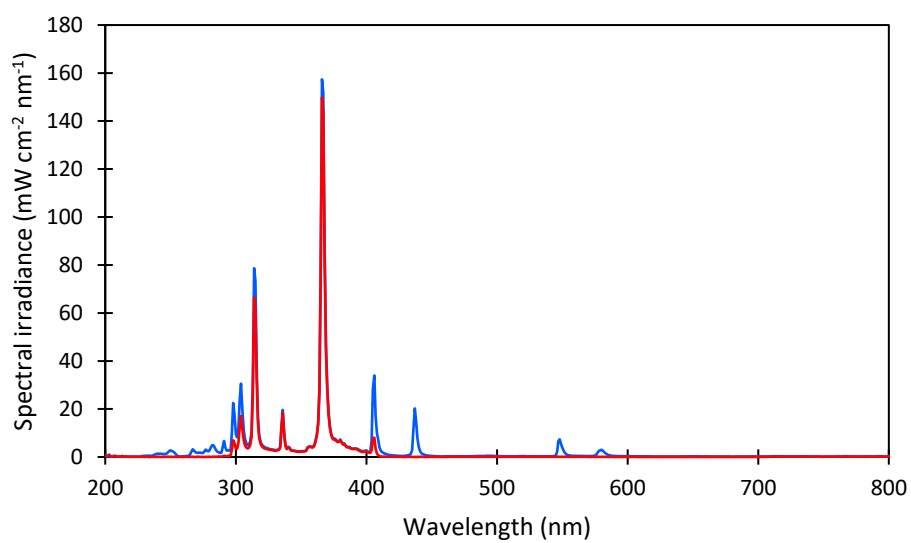


Figure S5. Spectrum of a Hg-Xe lamp (blue line) and that passed through an optical cutoff filter longer than 400 nm (short-pass, $\lambda > 400$ nm, red line).

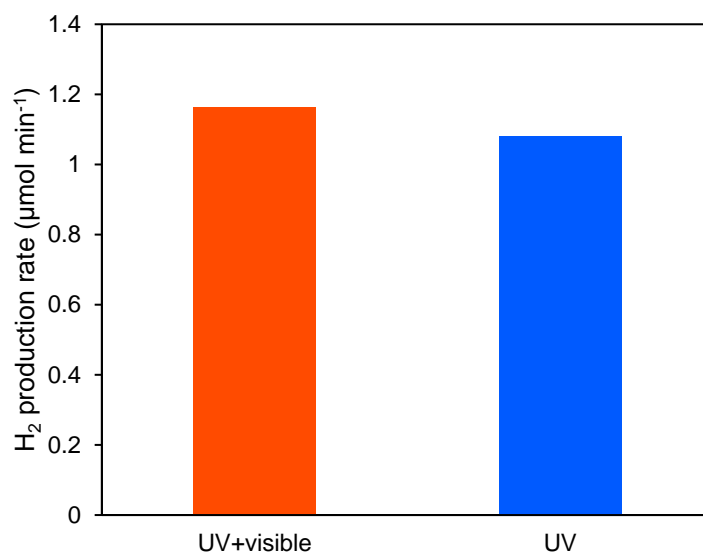


Figure S6. Hydrogen production rate under UV and visible light irradiation (orange bar) and that under UV irradiation only (blue bar). For both conditions, a Hg-Xe lamp was used, and the surface temperature was set at 442 °C by controlling the heater of the reactor. For the UV-only condition, a long cutoff filter (short-pass, $\lambda > 400$ nm) was used.

The hydrogen production rates were almost equal for both cases. In other words, if the surface temperature was the same, the DRM activity was the same regardless of whether visible light was included or not. These results indicate that the bandgap excitation under UV light is the dominant process to drive the DRM reaction.

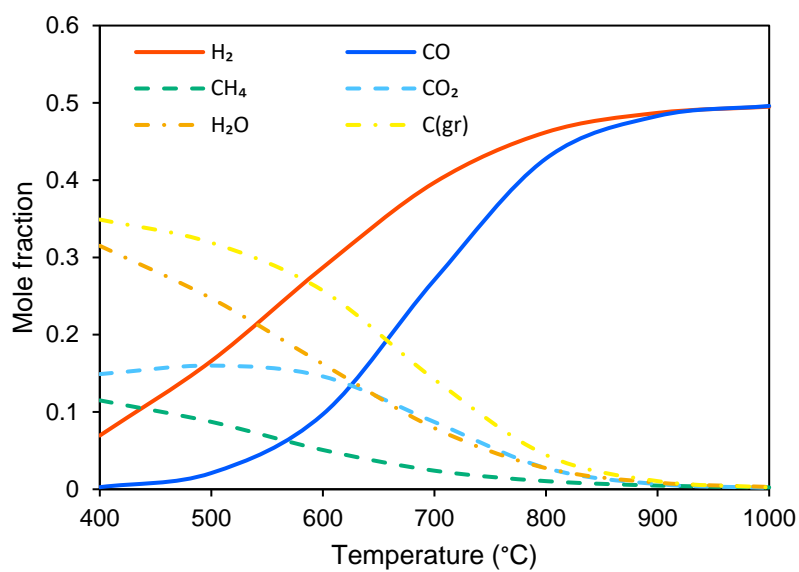


Figure S7. Temperature dependence on the gas composition under the thermodynamic equilibrium, which is calculated by CEA software (Calculation conditions: CH₄/CO₂ = 1, 1 atm).

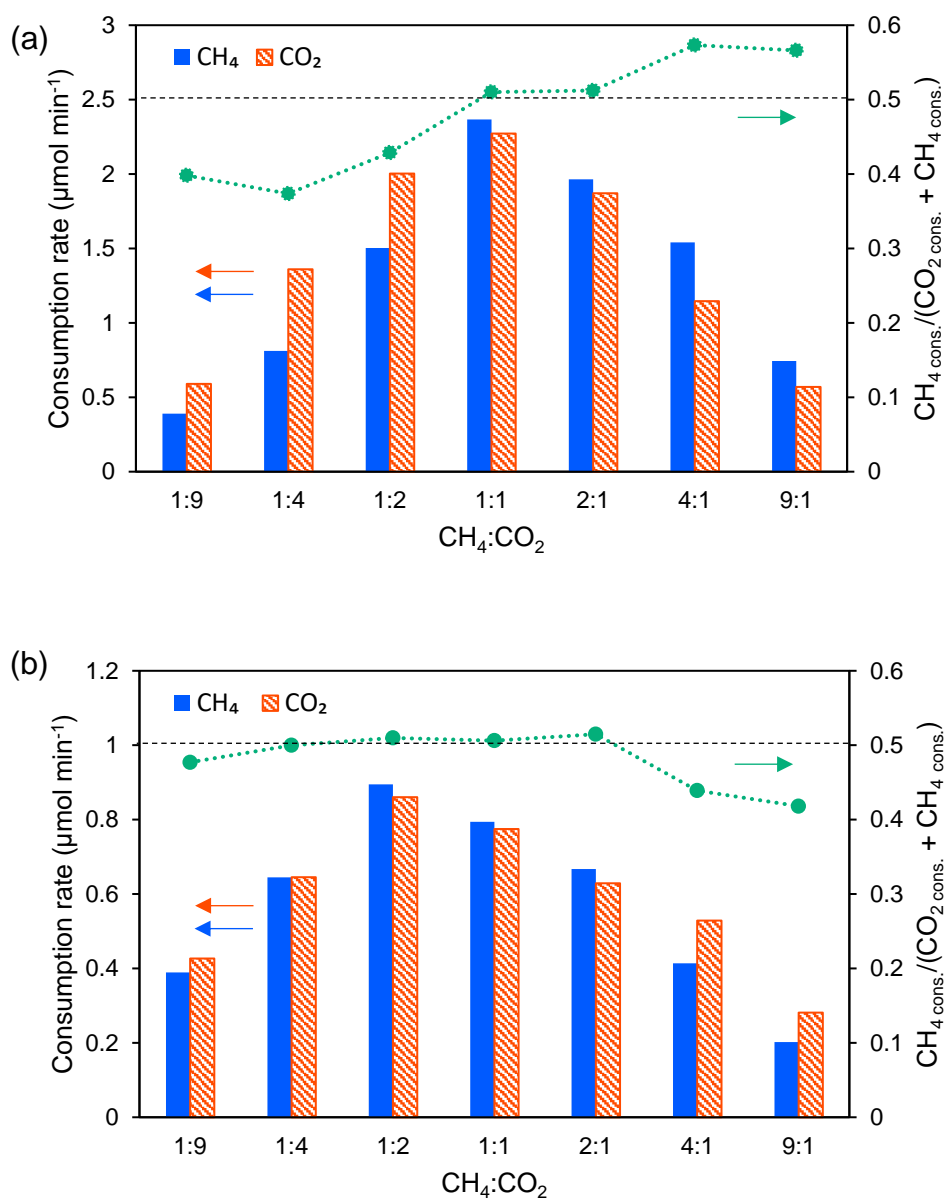


Figure S8. The consumption rates of CH₄ and CO₂ and the consumption rates ratio ($\text{CH}_4 \text{ cons.} / (\text{CO}_2 \text{ cons.} + \text{CH}_4 \text{ cons.})$) in each reactant gas composition under (a) dark at 800 °C and (b) light irradiation at 150 °C conditions, respectively.

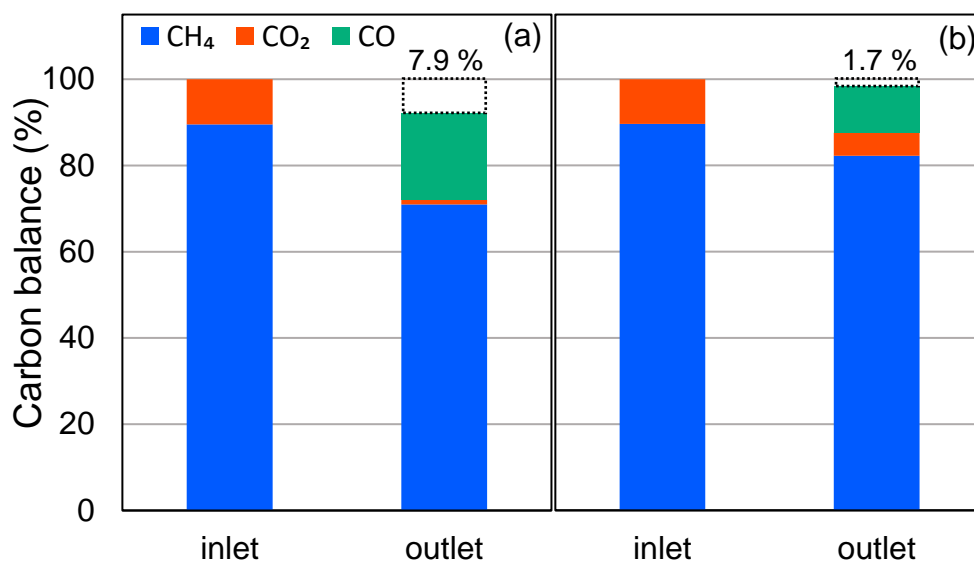


Figure S9. Carbon balance of the inlet and outlet gas during the reaction under (a) dark at 800 °C and (b) light at 150 °C conditions in CH₄/CO₂ = 9.

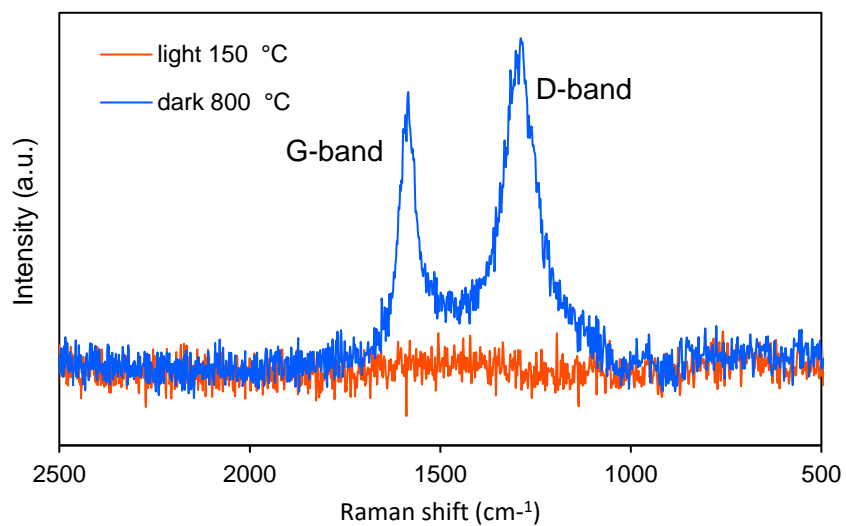


Figure S10. Raman spectra of the catalysts after being evaluated for 30 min in the dark (blue line) and light irradiation (red line) conditions under $\text{CH}_4/\text{CO}_2 = 9$ atmospheres.

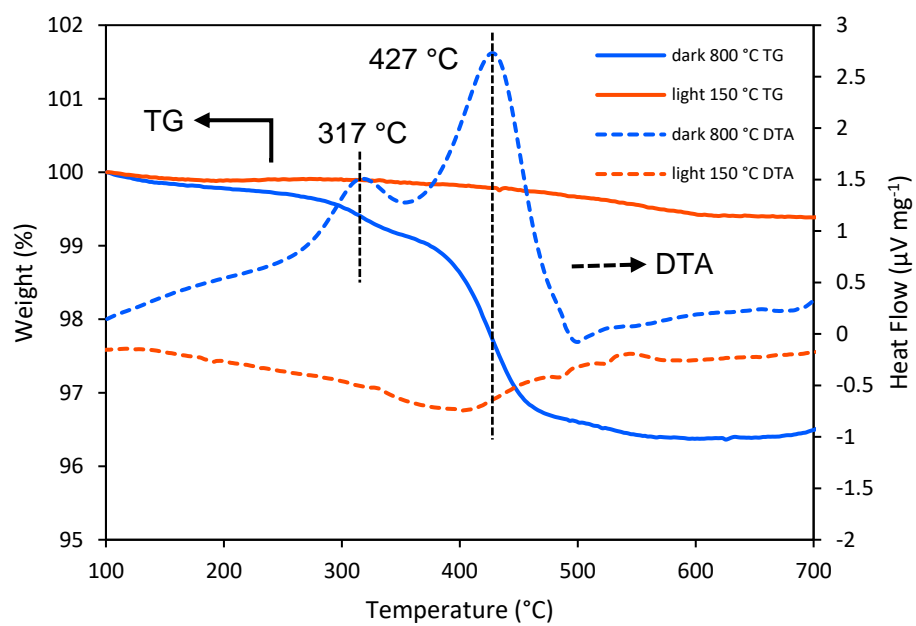


Figure S11. TG and DTA results of the catalysts after being evaluated for 30 min in dark and light irradiation conditions under $\text{CH}_4/\text{CO}_2 = 9$ atmospheres.

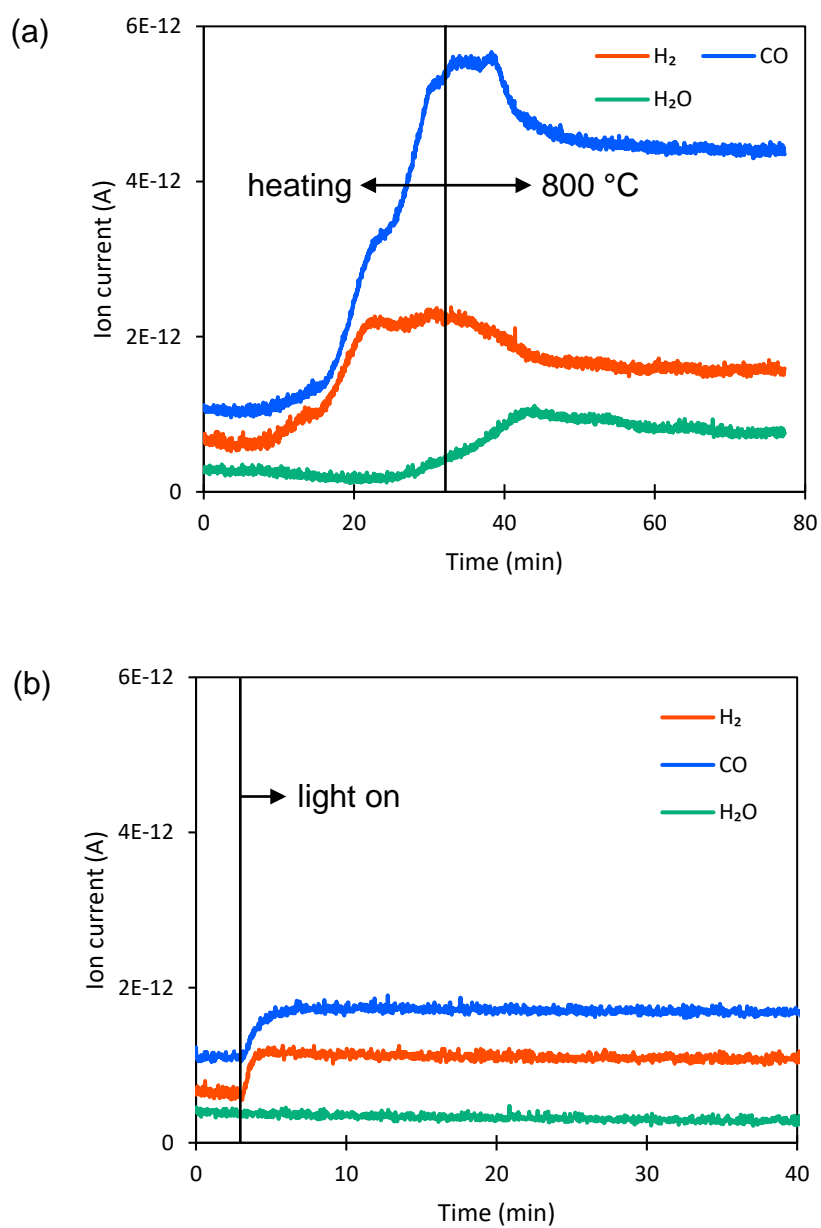


Figure S12. The time-on-stream Q-Mass signals during the DRM reaction in $\text{CH}_4/\text{CO}_2 = 1/9$. (a) under dark at 800 °C and (b) under light irradiation at 150 °C.